Breast Cancer Research

This Provisional PDF corresponds to the article as it appeared upon acceptance. Copyedited and fully formatted PDF and full text (HTML) versions will be made available soon.

Loss of BRCA1 leads to an increase in epidermal growth factor receptor expression in mammary epithelial cells, and epidermal growth factor receptor-inhibition prevents estrogen receptor-negative cancers in BRCA1-mutant mice

Breast Cancer Research 2011, **13**:R30 doi:10.1186/bcr2850

Laura N Burga (laura.burga@mcgill.ca)
Hai Hu (hhu@bidmc.harvard.edu)
Ashish Juvekar (ajuvekar@bidmc.harvard.edu)
Nadine M Tung (ntung@bidmc.harvard.edu)
Susan L Troyan (stroyan@partners.org)
Erin W Hofstatter (ehofstatter@bidmc.harvard.edu)
Gerburg M Wulf (gwulf@bidmc.harvard.edu)

ISSN 1465-5411

Article type Research article

Submission date 23 July 2010

Acceptance date 11 March 2011

Publication date 11 March 2011

Article URL http://breast-cancer-research.com/content/13/2/R30

This peer-reviewed article was published immediately upon acceptance. It can be downloaded, printed and distributed freely for any purposes (see copyright notice below).

Articles in *Breast Cancer Research* are listed in PubMed and archived at PubMed Central.

For information about publishing your research in *Breast Cancer Research* go to

http://breast-cancer-research.com/info/instructions/

© 2011 Burga *et al.* ; licensee BioMed Central Ltd.
This is an open access article distributed under the terms of the Creative Commons Attribution License (http://creativecommons.org/licenses/by/2.0), which permits unrestricted use, distribution, and reproduction in any medium, provided the original work is properly cited.

Loss of BRCA1 leads to an increase in epidermal growth factor receptor expression in mammary epithelial cells, and epidermal growth factor receptor-inhibition prevents estrogen receptor-negative cancers in BRCA1-mutant mice

Laura N Burga[1,2,^], Hai Hu[1,2,^], Ashish Juvekar[1], Nadine M Tung[1], Susan L Troyan[3], Erin W Hofstatter[1], Gerburg M Wulf[1,2,*]

1 - Division of Hematology/Oncology, Beth Israel Deaconess Medical Center, 330 Brookline Avenue, Boston MA 02215, USA

2 - Cancer Biology Program, Beth Israel Deaconess Medical Center, Brookline Avenue, Boston MA 02215, USA

3 – Department of Surgery, Brigham and Women's Hospital, Boston, MA 02115, USA

^ contributed equally

*corresponding author: gwulf@bidmc.harvard.edu

Abstract

Introduction

Women who carry a *BRCA1* mutation typically develop "triple-negative" breast cancers (TNBC), defined by the absence of estrogen receptor (ER), progesterone receptor (PR), and Her2/neu. In contrast to ER-positive tumors, TNBCs frequently express high levels of epidermal growth factor receptor (EGFR). Previously, we found a disproportionate fraction of progenitor cells in *BRCA1* mutation carriers with EGFR overexpression. Here we examine the role of EGFR in mammary epithelial cells (MECs) in the emergence of BRCA1-related tumors and as a potential target for the prevention of TNBC.

Methods

Cultures of mammary epithelial cells were used to examine EGFR protein levels and promoter activity in response to BRCA1 suppression with inhibitory RNAs. EGFR was assessed by immunoblotting, immunofluorescence, RT-PCR and flow cytometry. Binding of epidermal growth factor (EGF) to subpopulations of MECs was examined by Scatchard analysis. The responsiveness of MECs to the EGFR-inhibitor erlotinib was assessed *in vitro* in 3D-cultures and *in vivo*. MMTV-Cre BRCA1f/f;p53+/- mice were treated daily with erlotinib or vehicle control and breast cancer-free survival was analyzed using the Kaplan Meier method.

Results

Inhibition of *BRCA1* in mammary epithelial cells (MECs) led to upregulation of EGFR with an inverse correlation of *BRCA1* with cellular EGFR protein levels (r^2=0.87) and to an increase in cell surface expressed EGFR. EGFR upregulation in response to *BRCA1* suppression was mediated by transcriptional and post-translational mechanisms.

Aldehyde dehydrogenase-1 (ALDH1)-positive MECs expressed higher levels of EGFR than ALDH1-negative MECs, and were expanded 2 to 3-fold in the *BRCA1*-inhibited MEC population. All MECs were exquisitely sensitive to EGFR inhibition with erlotinib *in vitro*. EGFR-inhibition in MMTV-Cre *BRCA1*f/f p53+/- female mice starting at age 3 months increased disease-free survival from 256 days in the control to 365 days in the erlotinib-treated cohort.

Conclusions

We propose that even partial loss of *BRCA1* leads to an overall increase in EGFR-expression in MECs and to an expansion of the highly EGFR-expressing ALDH1-positive fraction. Increased EGFR expression may confer a growth advantage to MECs with loss of *BRCA1* at the earliest stages of transformation. Employing EGFR-inhibition with erlotinib specifically at this pre-malignant stage was effective to decrease the incidence of ER-negative breast tumors in this mouse model.

Introduction

Primary prevention of breast cancer has traditionally centered on estrogen receptor (ER) blockade, largely because the vast majority of breast cancers express ER and because ER-antagonists are both easily administered and well-tolerated. However, ER-antagonists do not prevent the most aggressive form of breast cancer: tumors that are ER-and PR-negative [1]. These tumors account for 15-20% of all breast cancers, occur with disproportionately high frequency in African-Americans and have the worst prognosis [2, 3]. The subgroup of women who are at highest risk for ER- and PR-negative breast cancers are women who carry a germline mutation in *BRCA1*. These women typically develop "triple-negative" breast cancers, which are defined by the absence of ER, PR and Her2 expression and are thought to be caused by genetic instability that results from a germ line mutation in *BRCA1* [4] .

Though nominally classified as a diagnosis of exclusion ("triple-negative"), these tumors frequently overexpress epidermal growth factor receptor (EGFR, 67%) whereas only a minority of ER-positive breast cancers overexpress EGFR (18%) [5, 6]. The high frequency of EGFR expression in triple-negative tumors suggests that loss of *BRCA1* may be coupled, either directly or indirectly, to EGFR overexpression in breast cancer [5]. This connection is further supported by the finding that sporadic triple-negative breast cancers frequently exhibit both epigenetic silencing of *BRCA1* [7] and overexpression of EGFR [6]. However, how triple-negative breast cancers enrich for tumor cells with high EGFR expression, is unknown. Previously, we examined the proliferation and differentiation properties of *BRCA1* mutant human primary MECs (HMECs) [8] and found a disproportionate fraction of progenitor cells in *BRCA1* mutation carriers with concomitant EGFR overexpression and absence of ER-α.

Here we report that inhibition of *BRCA1* in MECs leads to the upregulation of EGFR and the expansion of an aldehyde dehydrogenase-1 (ALDH1)-positive mammary epithelial progenitor cell population. We show that these MECs are exquisitely sensitive to EGFR inhibition with erlotinib, and that EGFR-inhibition *in vivo* could prevent the emergence of triple-negative breast cancers.

Materials and methods

Reagents*:* PE-conjugated mouse anti-EGFR (EGFR.1, 555997), PE-conjugated mouse IgG2b isotype control antibody (27-35; 555744) and QuantiBrite beads (340495) were from BD Biosciences; ALDEFLUOR assay kit was from StemCell Technologies; rhodamine-EGF (E-3481) was from Invitrogen. For immunofluorescence we used mouse anti-EGFR antibody (EGFR.1, 555997) from BD Biosciences. For immunohistochemistry we used anti-EGFR (ab52894) (Abcam, Rabbit monoclonal EP38Y), anti-ALDH1A1 (ab52492) (Abcam, Rabbit monoclonal, EP1933Y); anti-cleaved caspase 3 (CC3) (9661S, Cell Signalling, Rabbit polyclonal (Asp175)), anti-Ki67 (9106-S; Thermo Scientific, Rabbit monoclonal SP6), and mouse anti-ERα (MC-20; SC-524) from Santa Cruz. For immunoblotting mouse anti-*BRCA1* (MS110) was purchased from Calbiochem; erlotinib was purchased from LC Laboratories (Woburn, MA).

Cell culture: Informed consent was obtained for the collection of primary MECs from mastectomy specimen from BRCA1 mutation carriers (DFHCC-IRB legacy 04-405), and cells were isolated as described [8]. MECs were cultured in MEGM (Lonza) or HuMEC medium (Gibco, Invitrogen) supplemented with bovine pituitary extract. MCF10A (from ATCC), HMEC expressing hTERT and HMLE (gift from Dr. Robert Weinberg) were cultured in

DMEM-F12 medium (Dulbecco) supplemented with 5% horse serum, 20 ng/ml EGF, 0.5 mg/ml hydrocortisone, 100 ng/ml cholera toxin and 10 µg/ml insulin. MCF7 cells, HCC1937 *BRCA1*-mutant breast cancer cell line (from ATCC) and HCC1937 stably transfected with GFP-*BRCA1* (gift from Dr. Ralph Scully) were kept in RPMI1640 medium with 10% FBS. For 3-dimensional cultures, the cells were embedded in 40 µl of Geltrex (Gibco, Invitrogen) and cultured in 8-chamber culture slides (BD Falcon).

Cell Viability and Luciferase Assays: For cell viability assays, MECs were seeded at a density of 250/well in 96-well plates, and cell viability was determined using the Promega CellTiter-Glo® Luminescent Cell Viability Assay according to the manufacturer's instructions, and absorption was read using a Wallac 3 plate reader. For luciferase assays, HMEC or MCF7 cells were seeded in 24 well plates on day 1, transfected with BRCA1 si1 or si2 or control si RNA on day 2, and with control or the full-length EGFR luciferase construct on day 3, followed by luciferase assay on day 4. For each experiment, 2 µg of Reporter construct were transfected, in combination with either 1 (HMEC) or 10 ng (MCF7) of Renilla TK and luciferase activity was determined using a Wallac 3 plate reader.

Plasmids and inhibitory RNA constructs: The full-length EGFR-promoter inserted 5' from a luciferase reporter (Nishi H, Johnson AC, 2001) was a gift from Drs. Benjamin Purow and AC Johnson. The following sequences were used for the production of lentiviruses generating sh-RNA: CAGCAGTTTATTACTCACTAA (*Brca1* si1); CAGGAAATGGCTGAACTAGAA (*Brca1* si2); GCTAAACTCGTAATTCAACTT (scrambled control RNAi). Transient transfection of siRNAs was performed using siRNAs and HyperFect transfection protocol (Qiagen) according to the manufacturer's instructions. Stably infected cells lines were produced using lentiviruses. The sh-sequences were cloned into the pLKO.1 vector and

lentiviruses were produced in 293FT cell line. The cells were infected and selected with puromycin as previously described [9].

Flow Cytometry: To measure the kinetics of binding of EGF, cells were grown for 24 hours in 6 cm dishes, serum deprived for 4 to 6 hours at 37^{o}C, followed by 1 hour incubation on ice with indicated amounts of rhodamine-EGF. For uptake and binding, cells were incubated on ice with 10 ng of Rh-EGF, the excess rhodamine-EGF was removed with ice-cold PBS wash and the cells were incubated at 37^{o}C for the indicated intervals of time. The reaction was stopped on ice and the non-internalized receptor was stripped with a light acid buffer (50 mM glycine, 150 mM NaCl, pH 3.0). The cells were gently dissociated with trypsin replacement TrypLE (Gibco) and resuspended in PBS. The ALDEFLUOR kit (StemCell Technologies) was used to identify the stem and progenitor cell population, according to manufacturer's instructions. Bodipy-aminoacetaldehyde (BAAA) was used as a substrate, Diethylamino-benzaldehyde (DEAB) as inhibitor for negative controls. Cell surface bound EGFR was measured using a phycoerythrin (PE)-conjugated EGFR antibody and PE-conjugated mouse IgG2b isotype control antibody. Following gentle cell dissociation or ALDEFLUOR assay, the cells were washed, resuspended in 80 µl PBS/BSA or ALDEFLUOR assay buffer and 20 µl of either antibody or isotype control solution were added. Reactions were incubated on ice for 30 min, the cells were washed with PBS/BSA or ALDEFLUOR assay buffer and resuspended in 0.5 ml PBS or ALDEFLUOR assay buffer. QuantiBrite (BD Biosciences) beads were used to estimate the number of EGFR molecules per cell. Samples were measured with a Sorp 5-laser BDFASCS ARIA II or sorted using a MoFlo sorter (Dako).

Immunofluorescence: Cells cultured on cover slips for 24 hours were fixed for 10 min at room temperature in 3% paraformaldehyde/2%sucrose solution, rinsed twice with PBS and

permeabilized with ice-cold Triton X-100 solution (0.5% Triton X-100, 20 mM HEPES pH 7.4, 50 mM NaCl, 3 mM MgCl2, 300 mM sucrose) for 3 min on ice. The cells were rinsed for 5 times with PBS and blocked for 20 min with 10% goat serum followed by incubation with primary antibody anti-EGFR (EGFR.1) and anti-ALDH1A1 (EP1933Y) for 20 min at 37^{o}C. Cells were washed two times and incubated for 20 min at 37^{o}C with secondary antibody Alexa 488 conjugated anti-rabbit or Alexa 594 conjugated anti-mouse, dilution 1:1000 (Invitrogen). The nuclei were stained with DAPI, dilution 1:10000 and slides were examined using a Nikon Fluorescence Microscope. For the quantification of the fluorescence signal the mean intensity was determined using Image J software in 4 different fields for each sample. Experiments were performed in triplicate, and the mean and standard deviation of intensities were calculated for each condition.

Real Time RT-PCR: Total RNA was extracted using RNeasy Plus Mini Kit (Qiagen). RNA was reversely transcribed using the AccuScript enzyme (AccuScript High Fidelity RT-PCR System, Stratagene). Quantitative real-time PCR was carried out on a Rotor-Gene 6000, Corbett Research, using SYBR Green Supermix (Bio-Rad). The PCR reaction (15 μl) was performed under the following conditions: 95^{o}C for 10 min, followed by 45 cycles of 95^{o}C for 20 sec, 56^{o}C C for 25 sec and 72^{o}C for 40 sec. The expression of EGFR gene was normalized to GAPDH levels. The primer sequences for the human EGFR cDNA (70 bp) were forward primer, 5'-GCACCTACGGATGCACTGG-3' and reverse primer, 5'-GGCGATGGACGGGATCTTA-3'.

Immunohistochemistry, morphometry and statistics: Immunohistochemistry was performed as described previously [10]. Scoring for EGFR expression was done according to the following system: Score 0 No staining or staining in less than 10% of cells. Score 1+, a faint

perceptible membrane staining can be detected in more than 10% of cells. Score 2+, a weak to moderate complete membrane staining is observed in more than 10% of cells. Score 3+, a strong complete membrane staining is observed in more than 10% of the cells. Colonies were documented using ACT-1 software connected to an Olympus SZX12 or a Nikon EclipseS100 microscope and analyzed using SIGNATURE[8]. The two-sided t-test was used to determine significance. Kaplan-Meier analysis was done using the Graph Pad Prism Software package, and survival statistics were calculated using the log-rank test. Scatchard analysis of rhodamine-EGF binding was done as described previously [11, 12].

Animal experiments: All animal experiments were conducted in accordance to IACUC-approved protocols. Experiment female mice, *Brca1* flox/flox, MMTV-Cre, p53 +/-, were obtained by breeding *Brca1* conditional knockout mice from the NIH repository (01XC8,strain C57BL/6), originally generated by Drs. Xiaoling Xu and Chu-Xia Deng [13], who made these mice available to us via the NCI repository, with MMTV-Cre (Jackson Laboratory B6129-TgN(MMTV-Cre)4Mam)[14] and p53 knockout (Taconic Farms, P53N12-M, C57BL/6)[15]. At the time of the study mice had been inbred for 2 years (7 generations). The floxed or wild type status of *Brca1*, the presence of the MMTV-Cre transgene and the p53 heterozygosity were determined by PCR as previously described [13]. Mice were examined for the occurrence of tumors twice weekly. When tumormetrics were performed, the length and width of the tumor was determined using calipers, and the tumor volume was determined ($width^2$ x length/2). Tumor growth was recorded as ratio to tumor volume at diagnosis.

Results

***BRCA1* inhibition results in increased EGFR expression.** In order to examine whether EGFR up-regulation is directly related to the loss of *BRCA1*, we suppressed *BRCA1* in different MEC lines including MCF10A[16], HMEC-hTERT and HMLE [17]. These MEC lines have not yet undergone transformation, and instead are propagated as immortalized cells. HMEC were transfected with control or *BRCA1*-directed siRNA, and analyzed 72 to 120 hours after transfection. MCF10A and HMLE cells showed poor transfection efficiency upon transient transfection with siRNA, and therefore these cells were infected with lentiviruses that expressed small hairpin (sh) RNAi against *BRCA1* (Figure 1 A), and selected for pools of infected cells with puromycin. Asynchronously growing cells were lysed and analyzed for EGFR expression.
Throughout these experiments, the effects observed after short-term suppression of BRCA1 with transient transfection in HMEC were similar to the results obtained in MCF10A and HMLE cells with longer-term suppression of BRCA1 after lentiviral infection and puromycin selection.

In all three cell lines and with either approach, we found that EGFR protein levels as measured by immunoblotting with anti-EGFR antibodies, increased when *BRCA1* was inhibited (Figure 1 A). We measured the density of the immunoblotting signals and found that, with *BRCA1* inhibition, EGFR levels increased up to 5 times over baseline (Figure 1 A). In addition, there appeared to be a tight negative correlation of *BRCA1* and EGFR levels (r^2=0.87), suggesting a regulatory role of *BRCA1* for EGFR (Figure 1 B). Next, we examined EGFR levels in response to *BRCA1* suppression under conditions of steady state growth or serum starvation using immunofluorescence and quantification of the EGFR fluorescence signal (Figure 1 D, bar graph). We found that BRCA1 inhibition

led to EGFR up-regulation under both conditions, asynchronous growth and starvation, suggesting that the effect of *BRCA1* suppression on EGFR expression is not mediated by the absence or presence of growth factors (Figure 1 D).

We then used flow cytometry to examine if the increase in total cellular EGFR protein was accompanied by an increase in EGF binding sites on the cell surface as opposed to intracellular accumulation. We found that HMEC-hTERT expressed an average of 6 x 10^3 EGFR per cell, which increased up to 2-fold after siRNA inhibition of *BRCA1* (Figure 1 C). A similar increase of cell-surface EGFR was seen with a second BRCA1-targeted siRNA (si1) in HMEC and using BRCA1-directed shRNAs in MCF10A cells (Figure 4 G, H). Immunofluorescence of EGFR using anti-EGFR antibodies in HMEC-htert confirmed that *BRCA1* inhibition resulted in an increase in both surface and intracellular EGFR, with a strong increase of EGFR on the cell surface upon serum deprivation after *BRCA1* inhibition (Figure 1 D). In summary, we found that both transient and stable suppression of *BRCA1* led to an up to 5-fold increase in EGFR protein and, to an about 2-fold increase in the number of EGFR expressed on the MEC surface. Thus, the increase in intracellular EGFR was more pronounced than the increase in cell-surface-expressed EGFR upon *BRCA1* inhibition.

***BRCA1* inhibition increases EGFR expression through both an increase in transcription as well as stabilization of the EGFR protein.** We next examined the molecular mechanisms by which mechanisms *BRCA1* inhibition caused an increase in EGFR protein. Given earlier reports that *BRCA1* can function as a transcriptional regulator and specifically regulates another receptor tyrosine kinase, insuline-like growth factor-1 receptor (IGF-IR) [18, 19], we analyzed mRNA levels using quantitative RT-

PCR. We found that in MEC lines with stably suppressed *BRCA1* levels EGFR mRNA was up-regulated 1.5 to 2-fold in HMLE and 2 to 3-fold in MCF10A cells, indicating an increase in EGFR transcription in response to *BRCA1* down-regulation (Figure 2 A). We next examined the effects of BRCA1 suppression on EGFR promoter activity to determine if the increase in EGFR mRNA was due to direct transcriptional activation. As these luciferase assays required transient transfection of siRNA and reporter plasmid, they could only be performed in HMEC, not in MCF10A or HMLE cells. Therefore, we performed a second set of luciferase assays in MCF7 breast cancer cells. We found that EGFR promoter activity increased up to 2-fold upon BRCA1 suppression (Figure 2 B), consistent with the increase in mRNA levels observed (Figure 2 A), confirming that BRCA1 exerts a negative regulatory role on EGFR transcription..

Because *BRCA1* also has a ubiquitin-ligase activity towards tubulin [20], ER-α [21] and phosphorylated Akt [22], and because we observed a pronounced increase in intracellular EGFR upon BRCA1 suppression (Figure 1 D), we tested if *BRCA1* suppression affected EGFR stability after blockade of protein biosynthesis with cycloheximide (Figure 2 C, D). Interestingly, *BRCA1*-suppression increased the half-life of the EGFR protein from less than 30 min to over 75 min (Figure 2 D). Thus, there appear to be at least two mechanisms that result in an increase of EGFR protein upon *BRCA1*-suppression, transcriptional regulation as well as protein stabilization.

ALDH1-positive cells show an increase in EGFR expression. In immunofluorescence imaging, we noted heterogeneity with regard to EGFR expression in both, control MECs as well as in MECs after *BRCA1* inhibition (Figure1 D, Figure 3 D). An increased expression of EGFR in basal cells has previously been observed in mice [23] and human MECs [24] and a

drift towards high EGFR expression was seen in cell line models of basaloid breast cancer [25], which led us to examine if the EGFR levels differed between stem and non-stem cells, as defined by the expression of aldehyde-dehydrogenase 1 (ALDH1) [26, 27]. We found that mean numbers of EGFR were higher in the ALDH1-positive fraction of MECs than in the ALDH1 negative fraction. (Figure 3 A, upper panel, Figure 4 G). Consistently, ALDH1-positive MECs showed an increased binding of rhodamine-labeled EGF when compared to the ALDH1-negative fraction (Figure 3A, lower panel, B, C). Given these differences in cell-surface expressed EGFR, we compared the kinetics of EGF binding and internalization between ALDH1-positive and ALDH1-negative MECs. For the binding assay, cells were incubated with increasing concentrations of Rhodamine-labeled EGF, and binding was analyzed using flow cytometry (Figure 3B). Scatchard analysis of rhodamine-EGF binding at 4^{o}C showed that both, the ALDH1-positive and ALDH1-negative population, bound EGF with similar affinity (KD 0.32 nM) (Figure 3 B, insert). For binding and internalization (Figure 3C), cells were pre-incubated with rhodamine-EGF at 4^{o}C to allow for binding, followed by removal of unbound rhodamine-EGF, incubated for the indicated times and concentrations with Rh-labeled EGF at 37^{o}C, and then washed with either PBS or an acidified buffer as described previously [28], followed by ALDH1 stain. While the PBS wash removes only unbound rhodamine-EGF, the acidified buffer removes both, receptor-bound and unbound EGF, i.e. fluorescence after the acidic wash is representative of internalized EGF. We found that EGF binding was bi-phasic, both in ALDH1-positive and ALDH1-negative cells, with an initial saturation of EGF binding sites after 5 min, followed by a second, slower phase of binding and internalization. Internalization was complete after 30 min at 37^{o}C (Figure 3 C).

In summary, binding and internalization kinetics were similar in ALDH1-positive and ALDH1-negative MECs, while the total number of circulating EGFR was increased in the ALDH1-positive fraction.

***BRCA1* inhibition increases EGFR expression in both the ALDH1-negative and the expanded ALDH1-positive cell pool.** The heterogeneity of the MEC pool, and how this heterogeneity is affected by the loss of *BRCA1*, is an area of active research [27, 29]. Several immunophenotypic profiles have been used to define MEC progenitor cells, such as the CD24low/CD44high profile ([30] and the CD49f+/EpCam+ profile [29]. Consistent with the data of Liu et al. [27] and with our own observations in *BRCA1* mutation carriers [10], we found that the percentage of ALDH1-positive cells increased 4-fold in HMEC-hTERT and doubled in MCF10A cells in response to inhibition of *BRCA1* (Figure 4 C, F). In addition, we found a corresponding increase in the CD24low/CD44 high population in both HMLE and MCF10A cells expressing BRCA1 shRNA (Figure S1 in Additional file 1), thus confirming an increased MEC progenitor cell pool in response to BRCA1 inhibition [27, 30]. Using two-color flow cytometry and the Quantibrite system [31], we found that ALDH1-positive MECs carried 2 to 3-times the number EGFR as ALDH1-negative cells (Figure 3 A, 4 G, H). Upon *BRCA1* inhibition with siRNA in HMEC or with shRNA in MCF10A cells, a significant increase of EGFR was observed in ALDH1-negative and ALDH1-positive MECs (Figure 4 G, H, dark bars). Thus, our data show that *BRCA1* inhibition affects EGFR expression in two ways: *BRCA1* suppression leads to the expansion of the highly EGFR-expressing ALDH1-positive MEC pool (Figure 4 C, F, G, H), and, secondly, *BRCA1* inhibition raises the numbers of EGFR per cell in all MECs (ALDH1-positive and ALDH1-negative cells) likely through transcriptional activation (Figure 2 A) and post-translational mechanisms (Figure 2 B)

EGFR-inhibitor erlotinib blocks the outgrowth of normal and *BRCA1*-deficient MECs. Given our findings of EGFR upregulation in MECs upon *BRCA1* inhibition, and our previous findings of altered growth and differentiation patterns of EGFR-expressing MECs isolated from *BRCA1* mutation carriers [8], we asked if EGFR inhibition could block this phenotype. First, we examined the growth characteristics of control and *BRCA1*-suppressed or *BRCA1* mutant MECs. Consistent with our previous data, we found that MECs after experimental suppression of *BRCA1* formed larger colonies with greater efficiency than control cells in the three-dimensional matrigel-based cultures (Figure 5 A, B). Similar findings were obtained with primary MECs from *BRCA1* mutation carriers which yielded a higher number of larger colonies than controls (Figure 5 C and [8]). Finally, our results were further confirmed with MEC cultures from MMTV-Cre *BRCA1*f/f mice, where even the heterozygote loss of *BRCA1* led to increased clonality of MECs (Figure 6 B). Thus, our data in primary human MECs, murine MECs and in immortalized MECs with experimental *BRCA1* suppression all confirm that even partial suppression or heterozygote loss of *BRCA1* causes an increase in the clonogenicity and proliferative potential of MECs.

Next, we treated MECs with the EGFR-inhibitor erlotinib, and found that erlotinib efficiently blocked the outgrowth of colonies from all MECs, controls as well as *BRCA1*-suppressed MEC (Figure 5 A,B), of normal and *BRCA1*-mutant primary MECs (Figure 5 C) as well as of murine mammary epithelial that were wild-type or *BRCA1*-deficient (Figure 6 C). In dose-response experiments, we found that <1 μM erlotinib was sufficient to suppress MEC outgrowth in both human (Figure 5 D) and murine MECs (Figure 6 C), indicating that MECs carrying a wild-type EGFR are highly sensitive to the growth inhibitory effect of erlotinib. In addition, we used a MTT-based cell viability assay to determine the effects of erlotinib on

MEC growth. Cells were seeded at equal densities, and cell viability measured daily over a period of 7 days (Figure 5 E). This quantitative cell viability assay confirmed that both cell types that expressed BRCA1-inhibitory shRNA grew significantly faster, and reached double the cell number after 7 days of culture when compared to controls (Figure 5 E), thus confirming that loss of BRCA1 leads to accelerated proliferation of MECs. In the quantitative cell viability assay, MECs with loss of BRCA1 were equally sensitive to erlotinib as wild-type cells (Figure 5 E), confirming our observations in the colony formation assays (Figure 5 A, B, C, D and Figure 6). In summary, both read-out methods, colony formation assay as well as cell viability assay, confirmed that MECs with loss of BRCA1 that express higher EGFR levels proliferate more rapidly than controls, and that this increase in proliferation remains highly sensitive to the growth-inhibitory effect of Erlotinib.

MECs from *BRCA1* mutant mice show proliferation and differentiation patterns similar to MECs from human *BRCA1* mutation carriers. The model of MMTV-Cre flox-directed deletion of *BRCA1* was first developed by Drs. Xu and Deng [13] has been used extensively to examine *BRCA1*-related tumorigenesis. When grown in 3D matrigel-based cultures, murine MECs grew in patterns similar to human MECs, i.e. cells from wild-type mice formed hollow acini after a 10-14 day culture periods (Figure 6 A, upper panel). In cells isolated from MMTV-Cre *BRCA1*f/f p53+/- mice we found large, complex and solid structures (Figure 6 A, lower panel), similar to what we found in human *BRCA1* mutation carriers [8]. Next, we examined the mammary gland tissues of 5 MMTV-Cre BRCA1f/f-53+/- mice and 7 Cre-negative age-matched control mice for the expression of EGFR and ALDH1 (Figure 6 C). We found that the mammary glands of BRCA1-mutant mice in general contained more acini than the controls. In each of the MMTV-Cre BRCA1f/fp53+/- mammary glands we found entire

acini that stained positive for both EGFR and ALDH1, while only occasional, single cells were positive in any of the Cre-negative control glands.

MMTV-Cre *BRCA1*f/f p53+/- mice develop breast cancer with a latency of about 8 – 10 months, while MMTV-Cre *BRCA1*f/f mice develop tumors with relatively low penetrance beyond 1 year or older [32], and MMTV-Cre *BRCA1*f/wt mice rarely develop spontaneous breast cancers. Therefore, we examined the clonogenicity of murine MECs that had not yet formed tumors at age 7 months for MMTV-Cre *BRCA1*f/f p53+/- mice and at 12 months for MMTV-Cre *BRCA1*f/f or MMTV-Cre *BRCA1*f/wt. In comparison to wild-type cells, all three mutant cell types showed significantly increased colony formation (Figure 6 B). Interestingly, this increase in clonogenicity was observed not only in cells from mice with homozygote loss of *BRCA1*, but also cells from mice heterozygote loss of *BRCA1* (MMTV-Cre *BRCA1*f/wt), indicating that loss of a single allele, which is a situation analogous to a human *BRCA1* mutation carrier, already leads to an increase in colony formation (Figure 6 B).

Next, we examined if treatment with erlotinib was similarly effective in murine MECs as it was in human MECs, and we found that colony formation was suppressed effectively at 1 μM of erlotinib in the medium (Figure 6 D). Based on these findings we tested the efficacy of erlotinib for the primary prevention of breast cancer in *BRCA1*-mutant mice.

The EGFR-inhibitor erlotinib prevents the development of ER-negative, but not of ER-positive breast cancers in *BRCA1*-mutant mice. Starting at age 3 months, MMTV-Cre *BRCA1*f/f p53+/- mice were treated with either the EGFR inhibitor erlotinib at 100 mg/kg per day orally (treatment cohort) or vehicle control (control cohort), as dosed previously [33]. Endpoints were tumor-free survival and tolerability of the prophylactic erlotinib treatments. The mice tolerated the treatments well, the only adverse effect was

partial alopecia in about 30% of the mice. Mice were examined daily and tumors diagnosed by palpation. Upon necropsy, tumors were counted, fixed, and examined for estrogen receptor expression. Survival analysis (Figure 7) showed a median disease-free survival of 365 days in the erlotinib treated cohort versus 256 days in the control cohort, i.e. erlotinib treatments delayed tumor development by an average of 3 months. Only 19 tumors were observed in the erlotinib-treated cohort versus 31 tumors in the control cohort, a significant reduction ($p=0.0003$). Upon necropsy, tumors were fixed and processed for immunohistochemistry (Table 1 and Figure S2 in Additional file 2). As expected from previous studies [32, 34], the mice in the control cohort developed both ER-positive and ER-negative breast cancers, with a predominance of ER-negative tumors. Interestingly, while the number of ER-positive tumors was not significantly different in both cohorts, the number of ER-negative breast cancers was sharply reduced in the erlotinib-treated cohort (5 versus 19), indicating that erlotinib was effective in preventing the emergence of ER-negative, but not ER-positive breast cancers in this mouse model (Table 1). Importantly, EGFR staining showed that the erlotinib-treated cohort had a much lower number of EGFR-positive tumors than the control, again confirming that erlotinib treatments selected for EGFR-negative tumors (Table 1). ALDH1 stain was observed in nests and at the edges of the tumors in clusters (Figure S2 in Additional file 2), and was highly variable amongst tumors. There was a trend towards lower ALDH1 expression in the erlotinib-treated cohort, however given the high variability of ALDH1 expression significance was not reached. The Ki67 labeling index as a marker for proliferation [35] was also highly variable between tumors and did not differ significantly between the erlotinib-treated and control cohorts, although there was a

trend towards higher Ki67 expression in control tumors (Table 1). The cell death index as assessed by cleaved caspase 3 expression [35] was less variable, and we found a higher cell death index in the erlotinib treated cohort than in controls, possibly indicating that a fraction of the tumor cells still responded to EGFR-inhibition while the majority of tumor cells was resistant. Finally, we examined if erlotinib had any effect on the growth of established tumors in this mouse model (Figure 7 B). Tumor metrics showed that once tumors were established, erlotinib did not shrink these tumors, and tumors grew similarly to the vehicle-control treated tumors. The lack of efficacy of erlotinib on established turmos was seen in ER-negative or ER-positive tumors, further confirming that EGFR-inhibition prevented the emergence of ER-negative tumors, but likely did not kill nascent ER-negative tumors. In summary, we found that tumors that emerged in erlotinib-treated mice tended to be positive for estrogen receptor and negative for EGFR and ALDH1; once tumors were established, their growth was not delayed by treatments with erlotinib, indicating that the majority of tumor cells is resistant to erlotinib treatments and grows independent from EGFR-signaling.

Discussion

The haploinsufficiency phenotype of *BRCA1* includes enhanced proliferation of MECs.

We had previously found that that the non-malignant MECs from *BRCA1* mutation carriers contain a subpopulation of progenitor cells with significantly increased clonal and proliferative potential compared with normal controls [8]. 79% of these cells

had not undergone LOH but had remained heterozygote for *BRCA1* (ROH) and these cells tended to differentiate into ER-negative, EGFR-positive colonies when compared to controls. Our observations here confirm that even partial loss of *BRCA1* leads to an increase a MEC's ability for clonal proliferation (Figure 5, 6), lending further support to the concept that haplo-insufficiency of *BRCA1* with reduced protein levels of *BRCA1* leads to a differentiation block coupled with enhanced proliferation of MECs [8, 36].

***BRCA1* WT and *BRCA1* haploinsufficient MECs depend on EGFR for proliferation.** MECs rely on EGFR activation for migration, proliferation and survival of mammary epithelial progenitor cells. However, what role EGFR plays for either the initiation or the maintenance of the malignant phenotype is largely unknown. Regardless of whether the progenitor cell population expanded through the loss of *BRCA1* is defined by expression of ALDH1 [8, 27] or Epcam+/CD49+ [29] , the progenitor cell population expanded in *BRCA1* mutation carriers shows high EGFR expression relative to the control cells [8, 29]. Here we show that suppression of *BRCA1* directly leads to an increase in EGFR expression with increased clonal growth of MECs (Figure 5), which can be entirely suppressed by the EGFR-inhibitor erlotinib (Figure 5, 6,7), suggesting that while loss of BRCA1 leads to an increase in EGFR activity, loss of BRCA1 does not convey growth factor independence.

Multiple mechanisms contribute to the *BRCA1*-related increase in EGFR-expression. A direct regulatory role of *BRCA1* for the transcription of a receptor tyrosine kinase has been reported for the IGF-IR gene [18, 19, 37]. Werner et al. found that IGF-IR and IGF-IIR mRNA expression levels are elevated in tissues from women with a genetic predisposition to breast cancer [18, 19]. They showed that *BRCA1* interacts with

and prevents the binding of the transcription factor SP1 to the IGF-IR receptor. SP1 is a general transcription factor with a wide range of target promoters, amongst them EGFR [38]. Our data show that down-regulation of *BRCA1* directly increased EGFR mRNA as well as EGFR promoter activity, suggesting transcriptional regulation (Figure 2 A, B). Whether or not regulation of EGFR transcription is also mediated by binding of *BRCA1* to Sp1 is currently unclear. In addition, we showed a post-translational effect of *BRCA1* on EGFR protein stability (Figure 2 C, D). The fact that two independent mechanisms converge to increase cellular EGFR levels after *BRCA1* inhibition, suggests functional importance of this regulatory axis. *BRCA1* levels fluctuate throughout the cell cycle, and they are highest during S phase and mitosis [39]. Downstream signaling from EGFR, however, is tightly suppressed during mitosis, as tyrosine phosphorylation of EGFR is highest in G0/G1 phase and then gradually decreases during S and G2 phases and reaches its lowest levels during M phase [40]. Negative regulation of EGFR by *BRCA1* would ensure the temporal separation between phases when demand for mitogenic signaling is high, i.e. G0/G1, and phases when mitogenic signaling might interfere with DNA synthesis and repair, i.e. S-phase. Such regulatory loops might be dysfunctional in MECs that have lost one or both alleles of *BRCA1*, allowing for an increase in mitogenic signaling of MECs with inherent genetic instability and increased vulnerability to oncogenic transformation. In this scenario the primary effects of loss of *BRCA1*, i.e. an increase in genetic instability, would cooperate with the secondary effect, an increase in EGFR signaling, towards proliferation and eventual transformation of cells with increased genetic instability.

This BRCA1/EGFR cooperation concept could potentially be broadly applicable to mitogenic signaling, and might explain why not only EGFR but also IGF-IR [41] is increased in MEC that have lost *BRCA1*. It may also explain why *BRCA1* has a negative regulatory effect on the stability of phosphorylated Akt [22] and attenuates Erk-activation in response to estrogen or EGF stimulation [42, 43]. The hypothesis that even heterozygote loss of *BRCA1* may allow for an increase in mitogenic signaling and thereby convey a growth advantage to MECs with genetic instability is further supported by the fact that *BRCA1* mutation carriers have a strikingly high frequency of atypical ductal hyperplasia (ADH, 38% in *BRCA1* carriers vs. 4% in control tissues) and ductal carcinoma in situ (DCIS, 13% in *BRCA1* carriers versus none in control tissues) [44], which most often is negative for estrogen receptor (ER) and positive for EGFR [45].

EGFR-inhibition is effective for the prevention but not for the treatment of *BRCA1*-related breast cancers. The expression of the epidermal growth factor receptor (EGFR) in breast cancer has been linked to endocrine resistance and poor outcomes [46-48]. It has also been postulated that EGFR activation may be an important step in the progression to estrogen independence [49]. EGFR overexpression appears to correlate with the basaloid phenotype and is found in 67% of *BRCA1*-related cancers versus only 18% of non-*BRCA1*-related breast cancers [5]. These findings have prompted the launching of several clinical trials that examine the therapeutic efficacy of the EGF inhibitors gefitinib and erlotinib in estrogen-receptor negative breast cancer. Early outcome data do not point towards a major activity of EGFR inhibitors in unselected patients with metastatic breast cancer [50]. Similarly, pre-surgical exposure studies showed only modest or no activity of erlotinib on the proliferative index of triple-

negative breast cancers [51]. Our studies confirm that while erlotinib prevented the emergence of triple-negative breast cancers, manifest breast tumors grow independently from EGFR signaling (Figure 7 B).

EGFR-inhibition prevents the emergence of ER-negative but not of ER-positive breast cancers in *BRCA1*-mutant mice. Currently, there is a lack of non-surgical primary prevention options for women at risk for triple-negative breast cancer. Our data show that the EGFR-inhibitor erlotinib was effective for the prevention of EGFR-pos/ER-neg breast cancers, but not EGFR-neg/ER-pos breast cancers in *BRCA1* mutant mice (Figure 7, Tab 1). We have thereby demonstrated for the first time the principle that EGFR inhibition is effective in preventing *BRCA1*-related tumors. The concept of breast cancer prevention through EGFR inhibition has been explored previously; in fact, EGFR-inhibitors have been successfully used for the prevention of breast cancer in experimental mouse models [52-55]. However, these mice were BRCA1 proficient and at risk for breast cancer because of over-expression of transgenic erbB2 (Her2), which is a member of the EGFR family and a direct target for the drugs used in those studies, i.e. lapatinib or gefitinib. However, in humans, erbB2 amplification is the result of a somatic mutation. Thus, it is currently not possible to identify women at risk for the development of Her2-positive breast cancer, thereby limiting the applicability of these data. On the other hand, there is a need to develop medicinal strategies for the prevention of triple-negative breast cancer, especially in *BRCA1* mutation carriers, and our mouse model data suggest that targeting the EGFR pathway might be promising. While erlotinib has a relatively benign toxicity profile, the expected dermatological complications [56] and unknown longterm effects of this drug will likely still make it prohibitive to use this particular drug for

preventative purposes without time limits. A yet unsolved question is whether a shorter, limited period of time of EGFR inhibition would be protective beyond the actual treatment time, and we are planning to addres this issue in this mouse model. However, as increasingly naturally occurring compounds that suppress EGFR signaling are discovered, substances such as allophycocyanins might hold promise for use as chemopreventative agents [57, 58]. Our studies suggest that the window of opportunity for effective breast cancer prevention using EGFR-inhibitors is a state at which loss of *BRCA1* and gain of EGFR have occurred, but growth factor independence of cancer cells has not yet been established.

Conclusions

We have identified a cooperative effect of loss of BRCA1 with gain of EGFR expression that leads to increased clonal proliferation of MECs and may render these cells vulnerable to malignant transformation. This cooperative effect is achieved by both transcriptional up-regulation as well as post-translational stabilization of EGFR upon BRCA1 down-regulation. In addition, cells with loss of BRCA1 enrich for the highly EGFR-expressing ALDH1-positive population. The tumorigenic effect of the cooperation of loss of BRCA1 with gain of EGFR in non-malignant MECs can be disrupted by the preventative use of the EGFR-inhibitor erlotinib. Thus, at the pre-malignant stage EGFR-inhibition may provide a window of opportunity for breast cancer prevention.

Abbreviations

3D: three-dimensional; ADH: atypical ductal hyperplasia; ALDH1: aldehyde dehydrogenase 1 ; ATCC: American type culture collection ; BAAA: bodipyl-aminoacetaldehyde; BRCA1: Breast Cancer Gene 1; cDNA: complementary deoxyribonucleic acid; Cre : Cre recombinase; DAPI : 4',6-diamidino-2-phenylindole; DCIS: ductal carcinoma in situ; DEAB: diethylamino-benzaldehyde; EGF: epidermal growth factor; EGFR: epidermal growth factor receptor; EpCam: Epithelial Cell Adhesion Molecule; ER: estrogen receptor; Erk: extracellular signal-regulated kinases; f: floxed; FBS: fetal bovine serum; GFP: green fluorescent protein; HMEC: human mammary epithelial cells; IGF-IR: type I insulin-like growth factor receptor; IgG2b: immunoglobulin G 2 b; MEC: mammary epithelial cells; MMTV: mouse mammary tumor virus; mRNA: messenger RNA; MTT: 3-(4,5-dimethylthiazol-2-Yl)-2,5-diphenyltetrazolium bromide; PBS: phosphate buffered saline ; PCR: polymerase chain reaction; PE: phycoerythrin; PR: progesteron receptor; RenillaTK: renilla thymidin kinase; RNA: ribonucleic acid; RT-PCR: real-time polymerase chain reaction; Sh-RNA: small hairpin RNA; Si-RNA: small interfering RNA; SP1: specificity protein 1; TNBC: triple negative breast cancer; wt: wild type.

Competing interests

The authors declare that they have no competing interests.

Authors' contributions

GW, LB, HH, AJ and NT developed the concept and designed the experiments; ST, GW and LB isolated primary MECs; LB and HH performed the cell culture work; GW, LB

and AJ performed the mouse studies; GW, HH, LB, AJ and EH analyzed the data; GW, LB and EH wrote the manuscript. All authors read and approved the final manuscript.

Acknowledgements

We thank Drs. Lewis C. Cantley, Christina Gewinner, Susmu Kobayashi and Kun Ping Lu for their advice. We thank Drs. Xiaoling Xu and Chu-Xia Deng, who generated mice with the conditional BRCA1 mutation and made these available to us via the NCI repository. We thank Dr. Robert Weinberg for HMEC-hTERT and HMLE cells. We thank Dr. Mihnea Bostina for his adaptation of the Signature software package. We thank Drs. Benjamin Purow and AC Johnson for the EGFR-Luciferase construct.

Financial Support: This study and manuscript preparation were funded through research grants to the corresponding author (GW) from the Susan Komen Foundation (BCTR0601030), a Career Development Award through the Specialized Programs of Research Excellence in Breast Cancer CA089393 (NIH), a Concept Award from the Department of Defense (BC 046321) and a K08 Clinician Scientist Award (K08 CA093655-04, NIH). The funding agencies did not have a role in the collection, analysis, and interpretation of data; in the writing of the manuscript; or in the decision to submit the manuscript for publication.

References

1. Fisher B, Costantino JP, Wickerham DL, Cecchini RS, Cronin WM, Robidoux A, Bevers TB, Kavanah MT, Atkins JN, Margolese RG, Runowicz CD, James JM, Ford LG, Wolmark N: **Tamoxifen for the prevention of breast cancer: current status of the National Surgical Adjuvant Breast and Bowel Project P-1 study.** *J Natl Cancer Inst* 2005, **97:**1652-1662.
2. Cleator S, Heller W, Coombes RC: **Triple-negative breast cancer: therapeutic options.** *Lancet Oncol* 2007, **8:**235-244.
3. Trivers KF, Lund MJ, Porter PL, Liff JM, Flagg EW, Coates RJ, Eley JW: **The epidemiology of triple-negative breast cancer, including race.** *Cancer Causes Control* 2009, **20:**1071-1082.
4. Foulkes WD: **Clinically relevant biology of hereditary breast cancer.** *Semin Oncol* 2007, **34:**379-383.
5. van der Groep P, Bouter A, van der Zanden R, Siccama I, Menko FH, Gille JJ, van Kalken C, van der Wall E, Verheijen RH, van Diest PJ: **Distinction between hereditary and sporadic breast cancer on the basis of clinicopathological data.** *J Clin Pathol* 2006, **59:**611-617.
6. Collins LC, Martyniak AJ, Kandel MJ, Stadler ZK, Masciari S, Miron A, Richardson AL, Schnitt SJ, Garber JE: **Basal Cytokeratin and Epidermal Growth Factor Receptor Expression Are Not Predictive of BRCA1 Mutation Status in Women With Triple-negative Breast Cancers.** *Am J Surg Pathol* 2009.
7. Birgisdottir V, Stefansson OA, Bodvarsdottir SK, Hilmarsdottir H, Jonasson JG, Eyfjord JE: **Epigenetic silencing and deletion of the BRCA1 gene in sporadic breast cancer.** *Breast Cancer Res* 2006, **8:**R38.
8. Burga LN TN, Troyan SE, Bostina M, Miron A, Konstantinopoulos P, Fountzilas H, Spentzos D, Lee B and Wulf GM: **Altered Differentiation and Proliferation Properties of Primary Mammary Epithelial Cells (PMECs) from BRCA1 mutation Carriers.** *Cancer Res* 2009, **in press**.
9. Ben-Dor I, Itsykson P, Goldenberg D, Galun E, Reubinoff BE: **Lentiviral vectors harboring a dual-gene system allow high and homogeneous transgene expression in selected polyclonal human embryonic stem cells.** *Mol Ther* 2006, **14:**255-267.
10. Burga LN, Tung NM, Troyan SL, Bostina M, Konstantinopoulos PA, Fountzilas H, Spentzos D, Miron A, Yassin YA, Lee BT, Wulf GM: **Altered proliferation and differentiation properties of primary mammary epithelial cells from BRCA1 mutation carriers.** *Cancer Res* 2009, **69:**1273-1278.
11. Carraway KL, 3rd, Cerione RA: **Fluorescent-labeled growth factor molecules serve as probes for receptor binding and endocytosis.** *Biochemistry* 1993, **32:**12039-12045.
12. Schmitz G, Wulf G, Bruning T, Assmann G: **Flow-cytometric determination of high-density-lipoprotein binding sites on human leukocytes.** *Clin Chem* 1987, **33:**2195-2203.
13. Xu X, Wagner KU, Larson D, Weaver Z, Li C, Ried T, Hennighausen L, Wynshaw-Boris A, Deng CX: **Conditional mutation of Brca1 in mammary**

epithelial cells results in blunted ductal morphogenesis and tumour formation. *Nat Genet* 1999, **22:**37-43.
14. Wagner KU, Wall RJ, St-Onge L, Gruss P, Wynshaw-Boris A, Garrett L, Li M, Furth PA, Hennighausen L: **Cre-mediated gene deletion in the mammary gland.** *Nucleic Acids Res* 1997, **25:**4323-4330.
15. Donehower LA, Harvey M, Slagle BL, McArthur MJ, Montgomery CA, Jr., Butel JS, Bradley A: **Mice deficient for p53 are developmentally normal but susceptible to spontaneous tumours.** *Nature* 1992, **356:**215-221.
16. Miller FR, Soule HD, Tait L, Pauley RJ, Wolman SR, Dawson PJ, Heppner GH: **Xenograft model of progressive human proliferative breast disease.** *J Natl Cancer Inst* 1993, **85:**1725-1732.
17. Elenbaas B, Spirio L, Koerner F, Fleming MD, Zimonjic DB, Donaher JL, Popescu NC, Hahn WC, Weinberg RA: **Human breast cancer cells generated by oncogenic transformation of primary mammary epithelial cells.** *Genes Dev* 2001, **15:**50-65.
18. Abramovitch S, Glaser T, Ouchi T, Werner H: **BRCA1-Sp1 interactions in transcriptional regulation of the IGF-IR gene.** *FEBS Lett* 2003, **541:**149-154.
19. Maor SB, Abramovitch S, Erdos MR, Brody LC, Werner H: **BRCA1 suppresses insulin-like growth factor-I receptor promoter activity: potential interaction between BRCA1 and Sp1.** *Mol Genet Metab* 2000, **69:**130-136.
20. Parvin JD: **The BRCA1-dependent ubiquitin ligase, gamma-tubulin, and centrosomes.** *Environ Mol Mutagen* 2009, **50:**649-653.
21. Ma Y, Fan S, Hu C, Meng Q, Fuqua SA, Pestell RG, Tomita YA, Rosen EM: **BRCA1 regulates acetylation and ubiquitination of estrogen receptor-alpha.** *Mol Endocrinol*, **24:**76-90.
22. Xiang T, Ohashi A, Huang Y, Pandita TK, Ludwig T, Powell SN, Yang Q: **Negative Regulation of AKT Activation by BRCA1.** *Cancer Res* 2008, **68:**10040-10044.
23. Asselin-Labat ML, Shackleton M, Stingl J, Vaillant F, Forrest NC, Eaves CJ, Visvader JE, Lindeman GJ: **Steroid hormone receptor status of mouse mammary stem cells.** *J Natl Cancer Inst* 2006, **98:**1011-1014.
24. Burke PM, Wiley HS: **Human mammary epithelial cells rapidly exchange empty EGFR between surface and intracellular pools.** *J Cell Physiol* 1999, **180:**448-460.
25. Agelopoulos K, Greve B, Schmidt H, Pospisil H, Kurtz S, Bartkowiak K, Andreas A, Wieczorek M, Korsching E, Buerger H, Brandt B: **Selective regain of egfr gene copies in CD44+/CD24-/low breast cancer cellular model MDA-MB-468.** *BMC Cancer*, **10:**78.
26. Wright MH, Calcagno AM, Salcido CD, Carlson MD, Ambudkar SV, Varticovski L: **Brca1 breast tumors contain distinct CD44+/CD24- and CD133+ cells with cancer stem cell characteristics.** *Breast Cancer Res* 2008, **10:**R10.
27. Liu S, Ginestier C, Charafe-Jauffret E, Foco H, Kleer CG, Merajver SD, Dontu G, Wicha MS: **BRCA1 regulates human mammary stem/progenitor cell fate.** *Proc Natl Acad Sci U S A* 2008, **105:**1680-1685.

28. Schmidt-Glenewinkel H, Reinz E, Eils R, Brady NR: **Systems biological analysis of epidermal growth factor receptor internalization dynamics for altered receptor levels.** *J Biol Chem* 2009, **284:**17243-17252.
29. Lim E, Vaillant F, Wu D, Forrest NC, Pal B, Hart AH, Asselin-Labat ML, Gyorki DE, Ward T, Partanen A, Feleppa F, Huschtscha LI, Thorne HJ, Fox SB, Yan M, French JD, Brown MA, Smyth GK, Visvader JE, Lindeman GJ: **Aberrant luminal progenitors as the candidate target population for basal tumor development in BRCA1 mutation carriers.** *Nat Med* 2009, **15:**907-913.
30. Ginestier C, Hur MH, Charafe-Jauffret E, Monville F, Dutcher J, Brown M, Jacquemier J, Viens P, Kleer CG, Liu S, Schott A, Hayes D, Birnbaum D, Wicha MS, Dontu G: **ALDH1 is a marker of normal and malignant human mammary stem cells and a predictor of poor clinical outcome.** *Cell Stem Cell* 2007, **1:**555-567.
31. Pannu KK, Joe ET, Iyer SB: **Performance evaluation of QuantiBRITE phycoerythrin beads.** *Cytometry* 2001, **45:**250-258.
32. Brodie SG, Xu X, Qiao W, Li WM, Cao L, Deng CX: **Multiple genetic changes are associated with mammary tumorigenesis in Brca1 conditional knockout mice.** *Oncogene* 2001, **20:**7514-7523.
33. Higgins B, Kolinsky K, Smith M, Beck G, Rashed M, Adames V, Linn M, Wheeldon E, Gand L, Birnboeck H, Hoffmann G: **Antitumor activity of erlotinib (OSI-774, Tarceva) alone or in combination in human non-small cell lung cancer tumor xenograft models.** *Anticancer Drugs* 2004, **15:**503-512.
34. Ludwig T, Fisher P, Ganesan S, Efstratiadis A: **Tumorigenesis in mice carrying a truncating Brca1 mutation.** *Genes Dev* 2001, **15:**1188-1193.
35. Shah C, Miller TW, Wyatt SK, McKinley ET, Olivares MG, Sanchez V, Nolting DD, Buck JR, Zhao P, Ansari MS, Baldwin RM, Gore JC, Schiff R, Arteaga CL, Manning HC: **Imaging biomarkers predict response to anti-HER2 (ErbB2) therapy in preclinical models of breast cancer.** *Clin Cancer Res* 2009, **15:**4712-4721.
36. Furuta S, Jiang X, Gu B, Cheng E, Chen PL, Lee WH: **Depletion of BRCA1 impairs differentiation but enhances proliferation of mammary epithelial cells.** *Proc Natl Acad Sci U S A* 2005, **102:**9176-9181.
37. Shukla V, Coumoul X, Cao L, Wang RH, Xiao C, Xu X, Ando S, Yakar S, Leroith D, Deng C: **Absence of the full-length breast cancer-associated gene-1 leads to increased expression of insulin-like growth factor signaling axis members.** *Cancer Res* 2006, **66:**7151-7157.
38. Xu J, Thompson KL, Shephard LB, Hudson LG, Gill GN: **T3 receptor suppression of Sp1-dependent transcription from the epidermal growth factor receptor promoter via overlapping DNA-binding sites.** *J Biol Chem* 1993, **268:**16065-16073.
39. Chen Y, Farmer AA, Chen CF, Jones DC, Chen PL, Lee WH: **BRCA1 is a 220-kDa nuclear phosphoprotein that is expressed and phosphorylated in a cell cycle-dependent manner.** *Cancer Res* 1996, **56:**3168-3172.
40. Kiyokawa N, Lee EK, Karunagaran D, Lin SY, Hung MC: **Mitosis-specific negative regulation of epidermal growth factor receptor, triggered by a**

decrease in ligand binding and dimerization, can be overcome by overexpression of receptor. *J Biol Chem* 1997, **272:**18656-18665.
41. Maor S, Yosepovich A, Papa MZ, Yarden RI, Mayer D, Friedman E, Werner H: **Elevated insulin-like growth factor-I receptor (IGF-IR) levels in primary breast tumors associated with BRCA1 mutations.** *Cancer Lett* 2007, **257:**236-243.
42. Razandi M, Pedram A, Rosen EM, Levin ER: **BRCA1 inhibits membrane estrogen and growth factor receptor signaling to cell proliferation in breast cancer.** *Mol Cell Biol* 2004, **24:**5900-5913.
43. Yan Y, Haas JP, Kim M, Sgagias MK, Cowan KH: **BRCA1-induced apoptosis involves inactivation of ERK1/2 activities.** *J Biol Chem* 2002, **277:**33422-33430.
44. Kauff ND, Brogi E, Scheuer L, Pathak DR, Borgen PI, Hudis CA, Offit K, Robson ME: **Epithelial lesions in prophylactic mastectomy specimens from women with BRCA mutations.** *Cancer* 2003, **97:**1601-1608.
45. van der Groep P, van Diest PJ, Menko FH, Bart J, de Vries EG, van der Wall E: **Molecular profile of ductal carcinoma in situ of the breast in BRCA1 and BRCA2 germline mutation carriers.** *J Clin Pathol* 2009, **62:**926-930.
46. Klijn JG, Berns PM, Schmitz PI, Foekens JA: **The clinical significance of epidermal growth factor receptor (EGF-R) in human breast cancer: a review on 5232 patients.** *Endocr Rev* 1992, **13:**3-17.
47. Fox SB, Harris AL: **The epidermal growth factor receptor in breast cancer.** *J Mammary Gland Biol Neoplasia* 1997, **2:**131-141.
48. Rampaul RS, Pinder SE, Nicholson RI, Gullick WJ, Robertson JF, Ellis IO: **Clinical value of epidermal growth factor receptor expression in primary breast cancer.** *Adv Anat Pathol* 2005, **12:**271-273.
49. Gee JM, Hutcheson IR: **Understanding endocrine resistance: the critical need for sequential samples from clinical breast cancer and novel in vitro models.** *Breast Cancer Res* 2005, **7:**187-189.
50. Dickler MN, Cobleigh MA, Miller KD, Klein PM, Winer EP: **Efficacy and safety of erlotinib in patients with locally advanced or metastatic breast cancer.** *Breast Cancer Res Treat* 2009, **115:**115-121.
51. Guix M, Granja Nde M, Meszoely I, Adkins TB, Wieman BM, Frierson KE, Sanchez V, Sanders ME, Grau AM, Mayer IA, Pestano G, Shyr Y, Muthuswamy S, Calvo B, Krontiras H, Krop IE, Kelley MC, Arteaga CL: **Short preoperative treatment with erlotinib inhibits tumor cell proliferation in hormone receptor-positive breast cancers.** *J Clin Oncol* 2008, **26:**897-906.
52. Lu C, Speers C, Zhang Y, Xu X, Hill J, Steinbis E, Celestino J, Shen Q, Kim H, Hilsenbeck S, Mohsin SK, Wakeling A, Osborne CK, Brown PH: **Effect of epidermal growth factor receptor inhibitor on development of estrogen receptor-negative mammary tumors.** *J Natl Cancer Inst* 2003, **95:**1825-1833.
53. Li Y, Brown PH: **Prevention of ER-negative breast cancer.** *Recent Results Cancer Res* 2009, **181:**121-134.
54. Strecker TE, Shen Q, Zhang Y, Hill JL, Li Y, Wang C, Kim HT, Gilmer TM, Sexton KR, Hilsenbeck SG, Osborne CK, Brown PH: **Effect of lapatinib on the**

development of estrogen receptor-negative mammary tumors in mice. *J Natl Cancer Inst* 2009, **101:**107-113.
55. Lenferink AE, Simpson JF, Shawver LK, Coffey RJ, Forbes JT, Arteaga CL: **Blockade of the epidermal growth factor receptor tyrosine kinase suppresses tumorigenesis in MMTV/Neu + MMTV/TGF-alpha bigenic mice.** *Proc Natl Acad Sci U S A* 2000, **97:**9609-9614.
56. Rhee J, Oishi K, Garey J, Kim E: **Management of rash and other toxicities in patients treated with epidermal growth factor receptor-targeted agents.** *Clin Colorectal Cancer* 2005, **5 Suppl 2:**S101-106.
57. Afaq F, Zaman N, Khan N, Syed DN, Sarfaraz S, Zaid MA, Mukhtar H: **Inhibition of epidermal growth factor receptor signaling pathway by delphinidin, an anthocyanidin in pigmented fruits and vegetables.** *Int J Cancer* 2008, **123:**1508-1515.
58. Zhang Y, Vareed SK, Nair MG: **Human tumor cell growth inhibition by nontoxic anthocyanidins, the pigments in fruits and vegetables.** *Life Sci* 2005, **76:**1465-1472.

Figure legends

Figure 1 *BRCA1* suppression in MECs leads to an increase in EGFR. A. MECs were transfected with *BRCA1* control or siRNA, or infected with lentivirus expressing control or *BRCA1*-specific shRNAs and lysed for immunoblotting. B. The intensities of the ECL signal of EGFR, *BRCA1* and Tubulin levels were quantified using Image J software. C. Flow Cytometry using PE-conjugated anti EGFR antibodies show an increase of cell surface EGFR after *BRCA1* suppression (HMEC-hTERT, similar results were obtained with MCF10A). D. Immunofluorescence of EGFR in asynchronously growing MECs (HMLE), upper panel and after serum deprivation (lower panel) in control (left panel) and *BRCA1*-suppressed MEC cells (right panel). Experiments were performed in triplicates and using control and two different sh-containing MEC lines. Fluorescence intensity of the images was quantified using ImageJ software (bar graph, 1 D, right).

Figure 2 The increase in EGFR expression after *BRCA1* inhibition is caused by transcriptional (A, B) and post-translational mechanisms (C, D). A. EGFR mRNA levels were determined in control (light bars) and in MECs expressing shRNAs directed against *BRCA1* (dark bars). RNA levels were normalized for GAPDH expression. B. Decreased EGFR promoter activity as a result of short-term BRCA1 suppression in MECs and MCF7 cancer cells. BRCA1 control and siRNA and the full-length EGFR promoter were transfected as indicated, luciferase activity was normalized for Renilla-TK expression. C, D EGFR half-life increases from less than 30 min to over 70 min after *BRCA1* inhibition. Control and *BRCA1* sh2-expressing MCF10A cells were transfected with HA-tagged EGFR 48 hours prior to the time course, serum-deprived for 8 hours prior to maximize EGFR expression, treated with cycloheximide at 100 μcg/ml for 2 hrs, stimulated with EGF at point 0. Lysates were prepared and immunoblotted at the indicated time points. The ECL signal was quantified as in Figure 1B. Similar results were obtained with BRCA1 sh1-expressing cells.

Figure 3 Heterogeneity and kinetics of EGFR expression in MECs. A. Dual staining of ALDH1-positive cells (green fluorescence) with anti-EGFR antibodies (upper panel) or rhodamine-labeled EGF (lower panel) in HMEC-hTERT. The left panel shows negative controls used to adjust compensation settings. ALDH1-positive cells show higher EGF binding and a higher number of EGFR (right panels). B. Binding of EGF in ALDH1-negative or ALDH1-positive MECs. Cells were incubated at 4^{o}C with the

indicated amounts of EGF and labeled with ALDH1 reagent. Insert: Scatchard analysis of EGF binding. KDs were 0.32 nM for both the ALDH1+ and the ALDH1- fraction. C. EGF binding and uptake. Cells were incubated with 10 ng/ml of rhodamine EGF at 4^{o}C, free rhodamine-EGF was removed and MECs counterstained with ALDH1 reagent. To assess binding and uptake, cells were washed with PBS (solid symbols). To assess solely uptake, bound EGF was removed using an acetic acid wash (bordered symbols). D. Immunofluorescence (IF) of EGFR and ALDH1 in aysynchronously growing MEC (HMEC-hTERT).

Figure 4 *BRCA1* inhibition increases EGRR expression in both, the ALDH1-negative fraction and in the expanded pool of ALDH1-positive cells in MEC populations. Cells were either transfected with control or *BRCA1* siRNAs (A, B, C) or infected with lentiviruses expressing control or *BRCA1* shRNAs (D, E, F). Cells treated with the ALDH1 inhibitor DEAB served as controls (A, D). G, H *BRCA1* inhibition increases the expression of cell-surface-bound EGFR in HMEC-hTERT or MCF10A cells, in the ALDH1-negative and the ALDH1-positive fractions. Live cells were harvested and incubated with ALDH1 reagent followed by immunostain with PE-conjugated anti-EGFR antibodies and quantification of EGFR using the BD Quantibrite standards for PE.

Figure 5 *BRCA1* inhibition leads to increased colony formation and size that is completely blocked by EGFR inhibition. MECs expressing either control sh or *BRCA1*-directed sh-RNA (A, B) or primary MECs isolated from reduction

mammoplasties or BRCA1 mutation carriers (C,D) were seeded and photographed after 10 days of culture. All colony formation was completely suppressed when cells were grown in the presence of erlotinib at 2 μM (right panel of phase images for each cell type). (D) MEC growth is inhibited at concentrations as low as 0.5 μM of erlotinib. Cells were seeded at 5000/well, allowed to grow for 10 days in the presence of the indicated amounts of erlotinib and counted. (E) Cell viability assay of control and of BRCA1-shRNA expressing HMLE cells. Cells were seeded in triplicate in 96 well plates at 250 cells/well and cell viability was determined daily. Dotted line and open symbol represent control cells, closed symbols cells expressing BRCA1-directed shRNA. Black lines - vehicle control; blue lines - culture in the presence of 2.5 μM erlotinib; red line - culture in the presence of 5 μM erlotinib.

Figure 6 Growth and proliferation properties of MECs isolated from MMTV-Cre *BRCA1*- mutant mice are similar to MECs isolated from human BRCA1 mutation carriers. MEC were harvested and pladed as described previously [8] (A, B). Cultures from wildtype control mice resulted in round acinar structures (A, upper panel), whereas cultures from MMTV-Cre *BRCA1*f/f p53+/- mice showed complex and irregular features (A, lower panel). B The overall colony forming efficiency of murine *BRCA1*-mutant MECs is increased. Non-tumor bearing WT and MMTV-*BRCA1*f/f p53+/-MECs were compared at age 7 months, and non-tumor bearing mice from MMTV-Cre *BRCA1* f/w (heterozygous loss of *BRCA1*) MMTV-Cre *BRCA1*f/f were compared at age 12 to 13 months. C Mammary glands from MMTV-Cre BRCA1f/fp53+/- mice contain EGFR and ALDH1-positive acini. Immunohistochemistry for EGFR and ALDH1 was done on 5

BRCA1-mutant mammary glands and 7 Cre-negative controls. Representative images are shown at 20x. D erlotinib is active in suppressing the growth of murine MECs, from mice of wildtype (WT), MMTV-Cre *BRCA1*f/f or MMTV *BRCA1*f/f p53+/- background. All MECs were seeded in matrigel-based cultures, and photographed and analyzed for colony formation using Signature Software after 14 days of culture.

Figure 7 A Erlotinib prevents the emergence of ER- but not of ER+ breast cancers in MMTV-Cre *BRCA1*f/f/p53+/- mice. Virgin female mice were treated as controls or with erlotinib at 100 mg/kg via oral gavage once a day on 7 days/week. Tumors were recorded when they were first palpated. A Kaplan Meier graphing and analysis of disease-free survival were performed using the Graph Prism Software. B The growth of established breast cancers is not affected by erlotinib treatments. Mice that developed tumors in the control cohort were switched to erlotinib treatments, and the tumor volume relative to the tumor volume at diagnosis was plotted against treatment time. ER-status was determined after necropsy. The trendline for vehicle-control treated tumors was established based on tumor volumes of control mice.

Table 1. Clinicopathologic features of the observed tumors in the erlotinib-treated prevention cohort and controls

	Erlotinib N=13	Control N=14	p
Median disease-free survival (days)	365	256	0.0001
Number of tumors	19	31	0.0003
ER-positive tumors	14	12	n.s.
ER-negative tumors	5	19	0.0000002
EGFR*			
0	10	3	0.0004
1+	6	8	
2+	0	6	
3+	0	2	
ALDH1*	3.8%	9.0%	0.11 (n.s.)
(SD)	(2.8%)	(9.8%)	
Ki67*	21.4%	30.4%	0.6 (n.s.)
(SD)	(14%)	(17.7 %)	
Cleaved Caspase 3*	18.4%	10.6	0.018
(SD)	(8.6%)	(8.4%)	

* Only 16 tumors in the erlotinib-treated cohort and 19 tumors in the control cohort could be processed for EGFR, ALDH1, Cleaved Caspase 3 and Ki67, A two-sided T-test was performed to analyze significance.

Additional files

Additional file 1

Figure S1

Loss of BRCA1 leads to an increase in the CD24lowCD44high stem cell population in MECs. MCF10 A or HMLE MEC cell lines expressing either control or BRCA1-inhibitory shRNA constructs were examined for CD24 and CD44 expression using dual

color flow cytometry. Gates were set using isotype controls for the respective antibodies. Note that increase in CD24 and loss of CD44 were more pronounced in HMLE cells than MCF10 cells. However, in both cell lines inhibition of BRCA1 led to a notable increase in CD24lowCD44high cells (from 1.1 to 3.8 and 8% in MCF10 and from 2.6 to 9.2 and 11.6 % in HMLE cells respectively).

Additional file 2

Figure S2

Immunohistochemistry of tumors in the erlotinib prevention cohort or controls. ALDH1 staining tended to be cytoplasmic and occur in nests and clusters of cells, as well as at the edges of tumors. EGFR staining was seen at the cell membrane and to some extent cytoplasmic. Estrogen Receptor and Ki67 stains were nuclear, and anti-cleaved caspase 3 antibodies stained cells entirely.

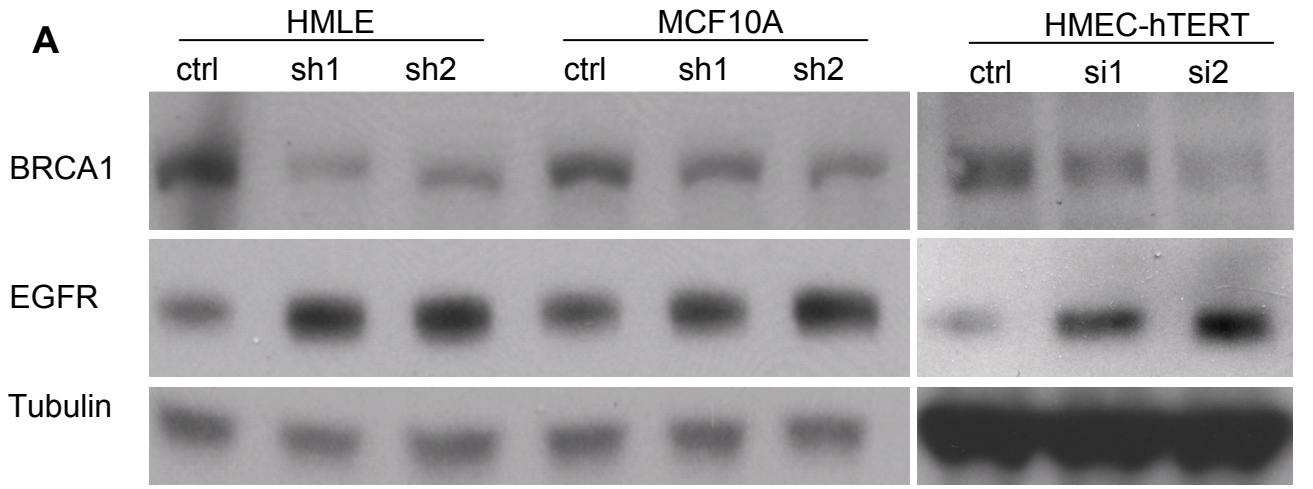

EGFR/Tubulin	1	6.2	4.4	1	1.5	2.7	1	3.9	5
BRCA1/Tubulin	1	0.2	0.2	1	0.6	0.6	1	0.5	0.05

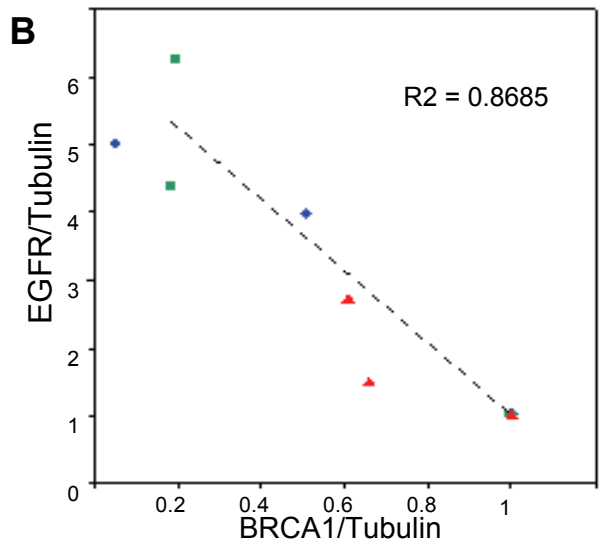

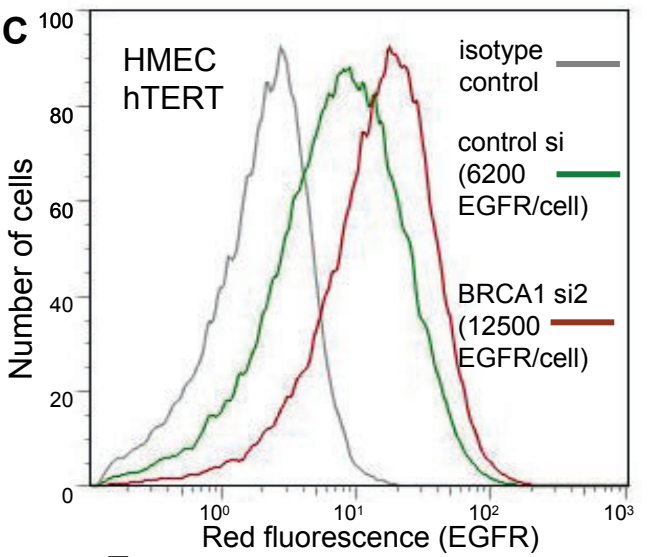

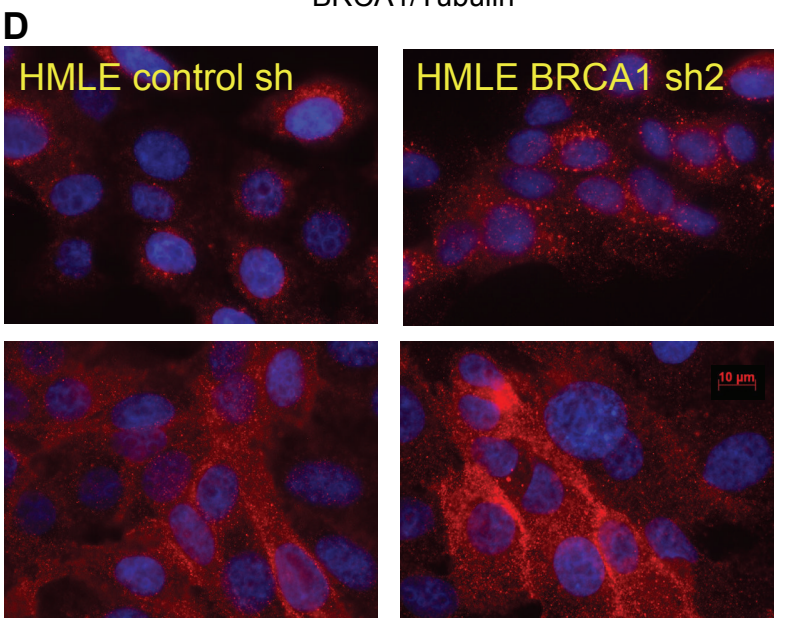

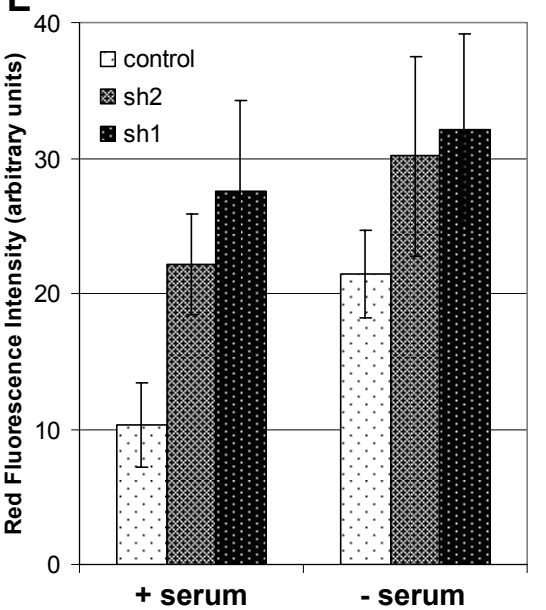

Figure 1

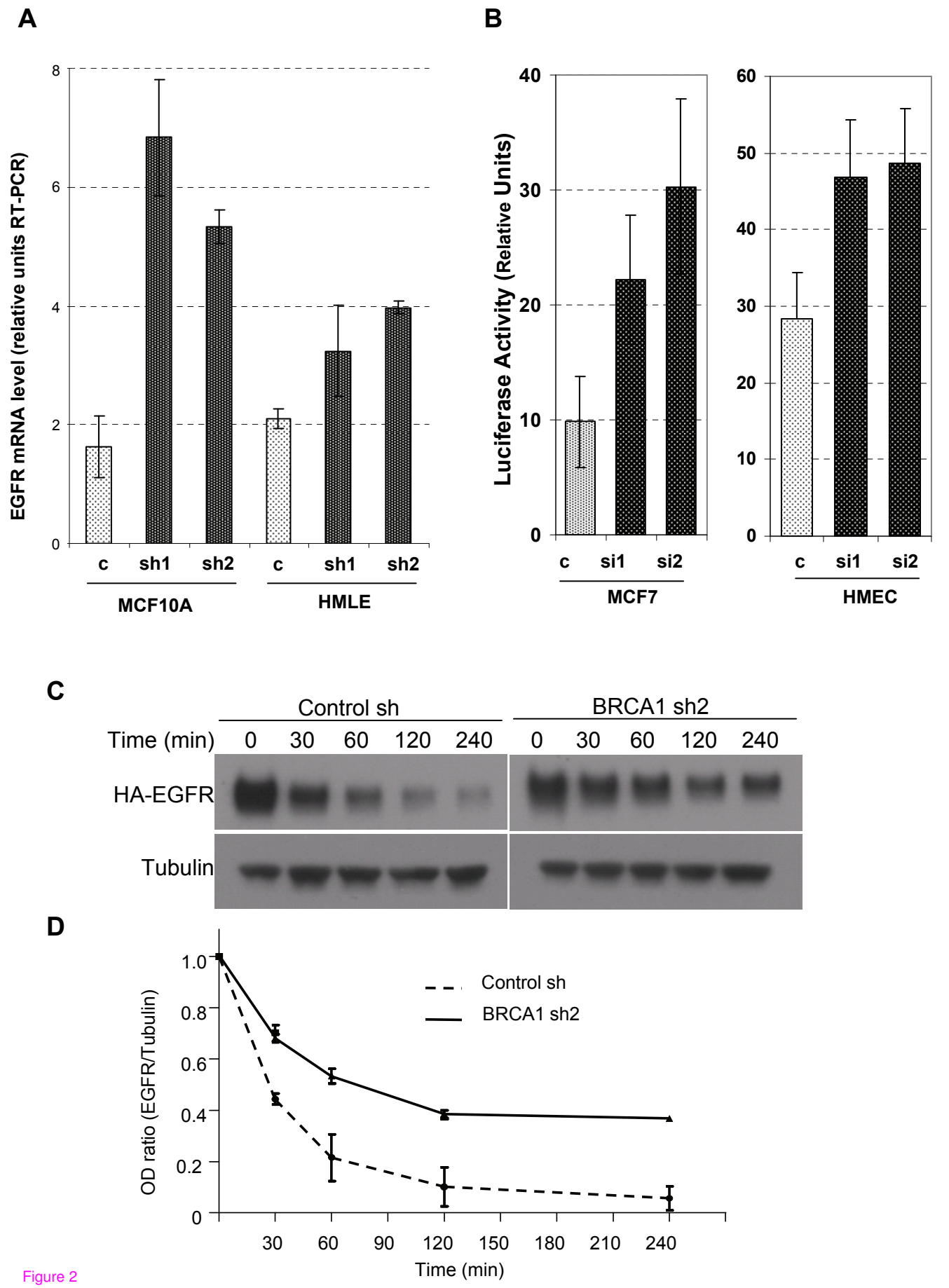
A
EGFR mRNA level (relative units RT-PCR)
8
6
4
2
0
c
sh1
sh2
c
sh1
sh2
MCF10A
HMLE
B
Luciferase Activity (Relative Units)
40
30
20
10
0
c
si1
si2
MCF7
60
50
40
30
20
10
0
c
si1
si2
HMEC
C
Control sh
BRCA1 sh2
Time (min)
0
30
60
120
240
0
30
60
120
240
HA-EGFR
Tubulin
D
OD ratio (EGFR/Tubulin)
1.0
0.8
0.6
0.4
0.2
0
Control sh
BRCA1 sh2
30
60
90
120
150
180
210
240
Time (min)

Figure 2

Figure 3

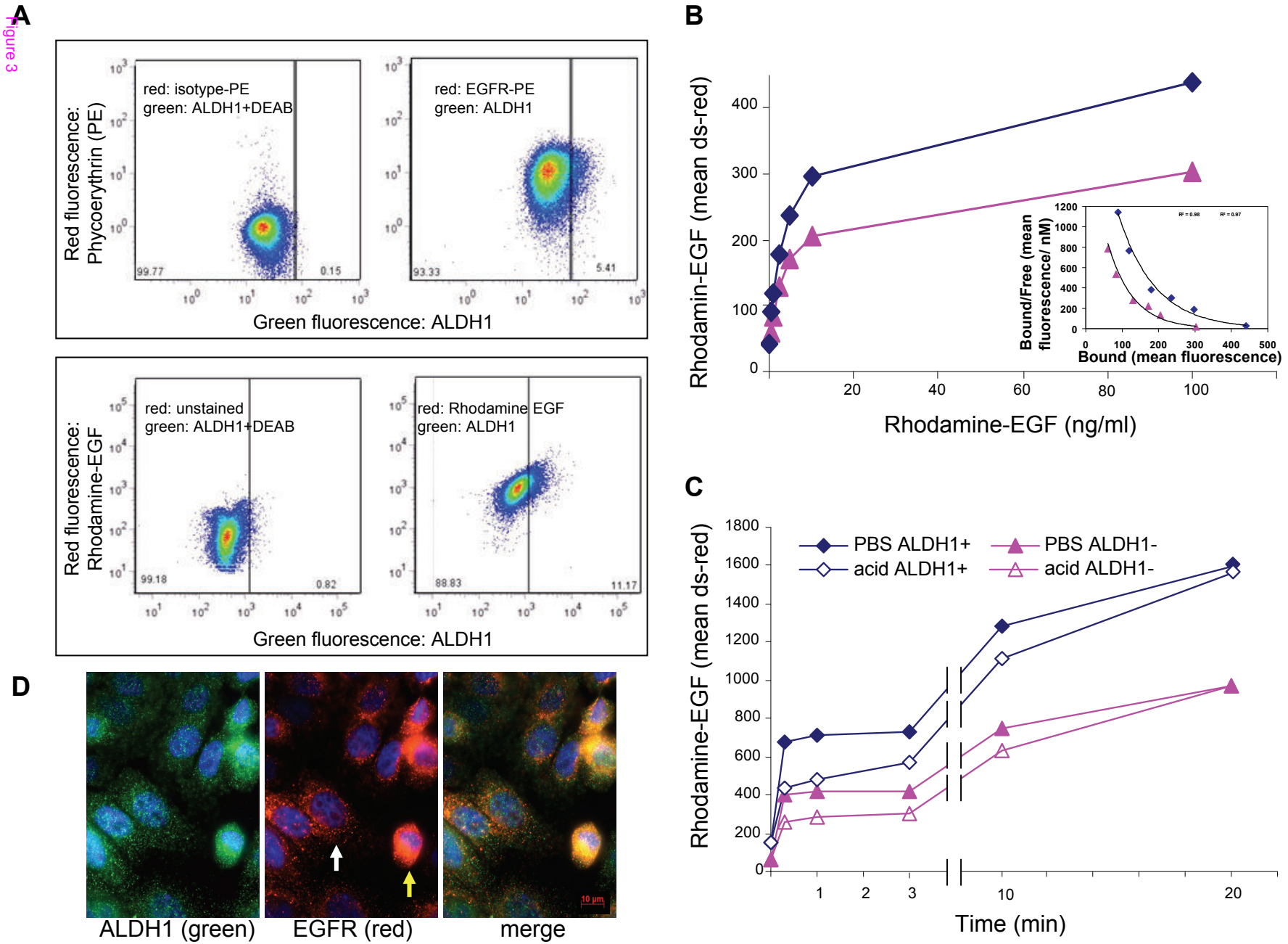
A
red: isotype-PE
green: ALDH1+DEAB
99.77
0.15
red: EGFR-PE
green: ALDH1
93.33
5.41
Red fluorescence: Phycoerythrin (PE)
Green fluorescence: ALDH1
red: unstained
green: ALDH1+DEAB
99.18
0.82
red: Rhodamine EGF
green: ALDH1
88.83
11.17
Red fluorescence: Rhodamine-EGF
Green fluorescence: ALDH1
B
Rhodamin-EGF (mean ds-red)
Rhodamine-EGF (ng/ml)
Bound/Free (mean fluorescence/ nM)
Bound (mean fluorescence)
C
PBS ALDH1+
acid ALDH1+
PBS ALDH1-
acid ALDH1-
Rhodamine-EGF (mean ds-red)
Time (min)
D
ALDH1 (green)
EGFR (red)
merge

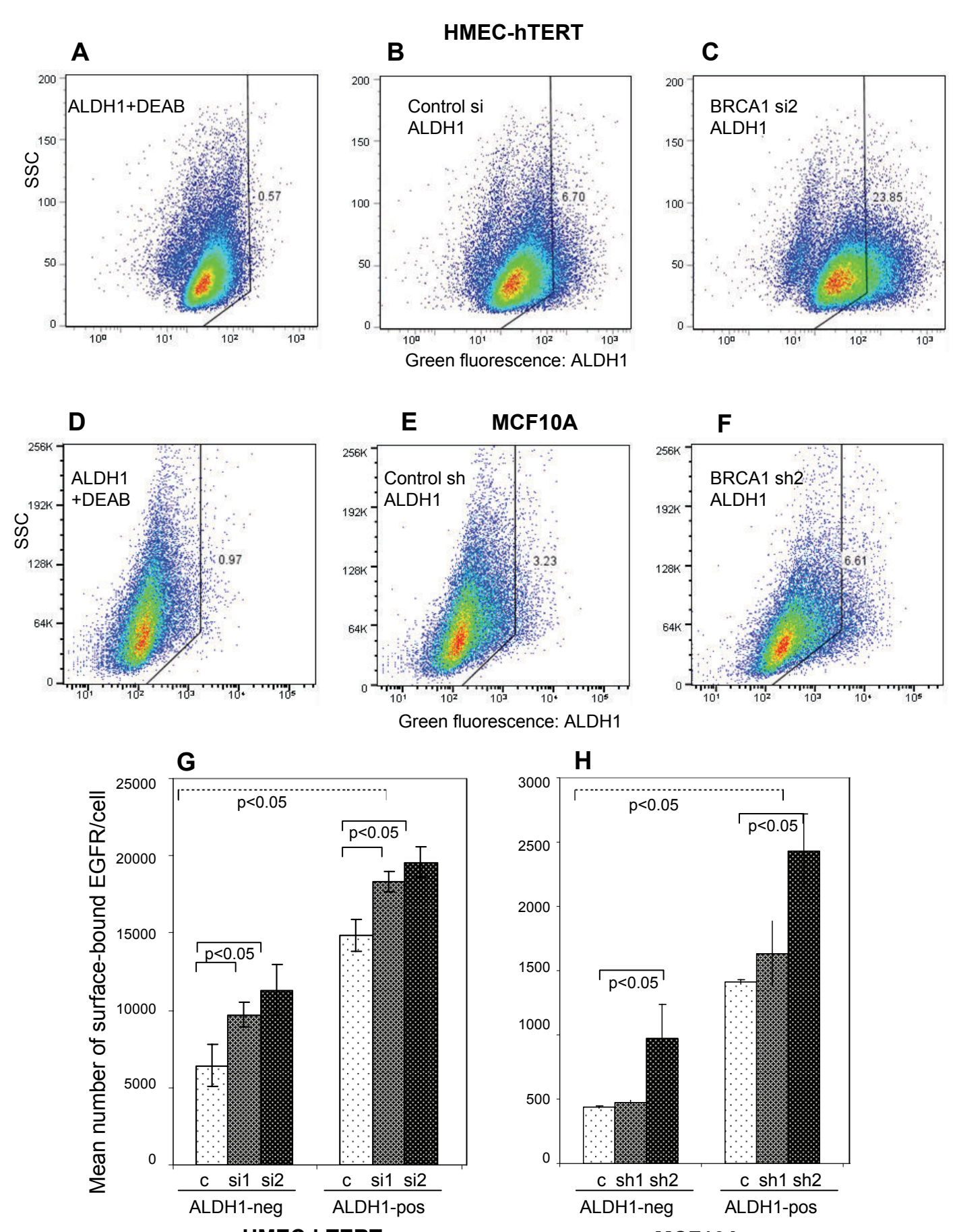
HMEC-hTERT
A
B
C
ALDH1+DEAB
Control si ALDH1
BRCA1 si2 ALDH1
SSC
0.57
6.70
23.85
Green fluorescence: ALDH1
D
E
MCF10A
F
ALDH1 +DEAB
Control sh ALDH1
BRCA1 sh2 ALDH1
0.97
3.23
6.61
Green fluorescence: ALDH1
G
H
Mean number of surface-bound EGFR/cell
p<0.05
c si1 si2
ALDH1-neg
ALDH1-pos
HMEC-hTERT
c sh1 sh2
MCF10A

Figure 4

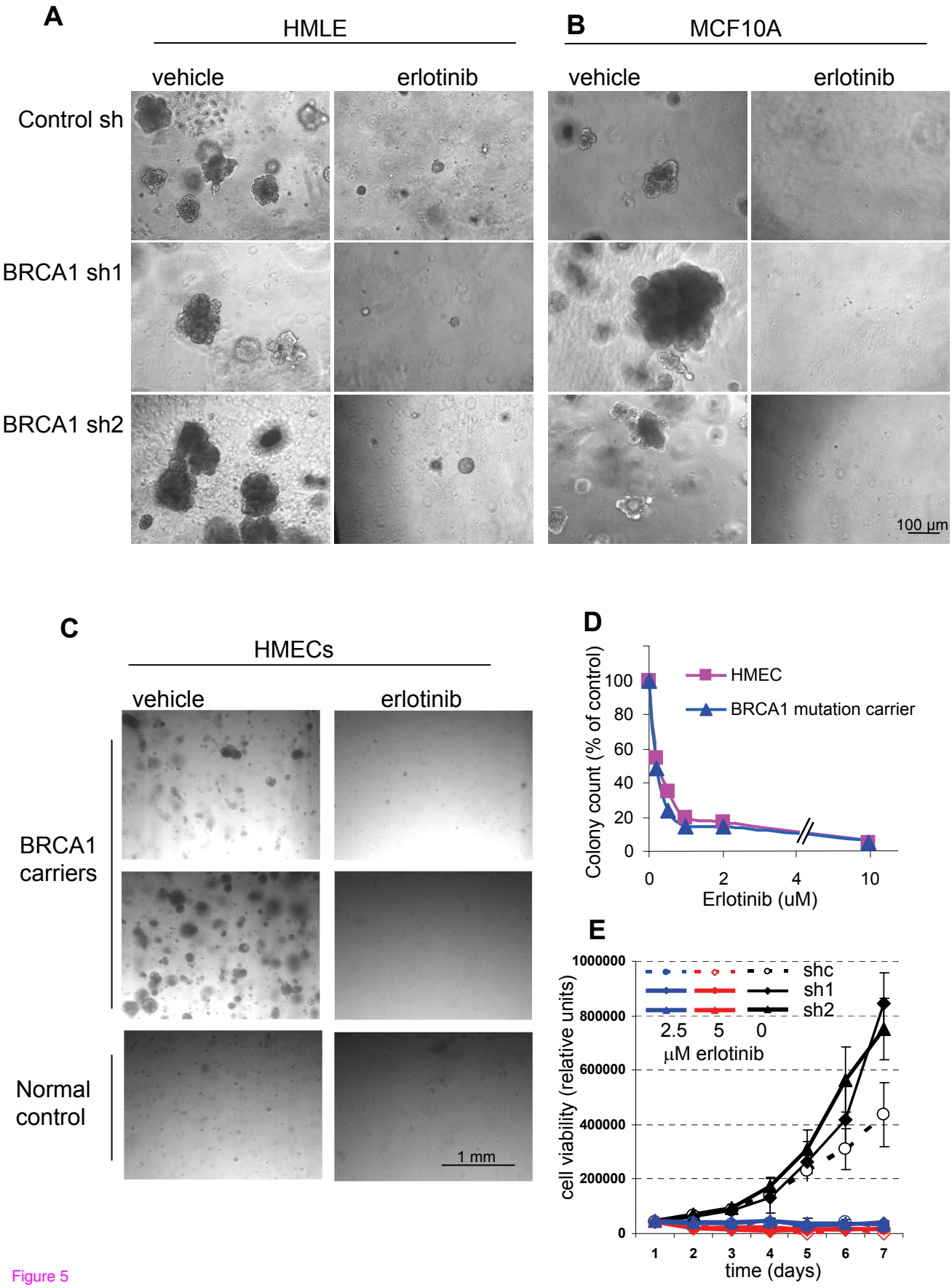
A
HMLE
vehicle
erlotinib
Control sh
BRCA1 sh1
BRCA1 sh2
B
MCF10A
vehicle
erlotinib
100 µm
C
HMECs
vehicle
erlotinib
BRCA1 carriers
Normal control
1 mm
D
HMEC
BRCA1 mutation carrier
Colony count (% of control)
100
80
60
40
20
0
0
2
4
10
Erlotinib (uM)
E
shc
sh1
sh2
2.5
5
0
µM erlotinib
cell viability (relative units)
1000000
800000
600000
400000
200000
0
1
2
3
4
5
6
7
time (days)

Figure 5

Figure 6

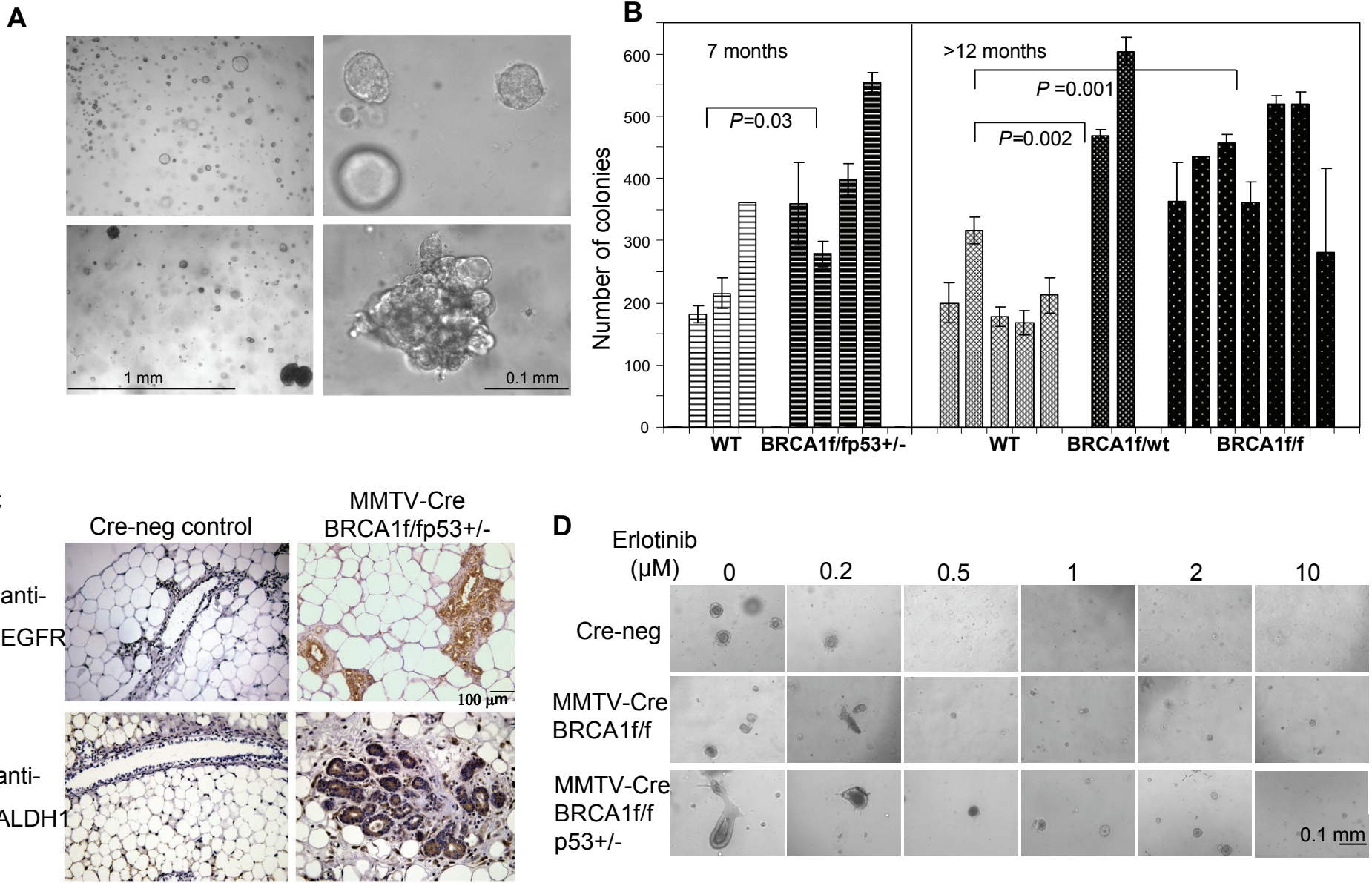
A
1 mm
0.1 mm
B
7 months
>12 months
P=0.03
P=0.002
P=0.001
Number of colonies
0
100
200
300
400
500
600
WT
BRCA1f/fp53+/-
WT
BRCA1f/wt
BRCA1f/f
C
Cre-neg control
MMTV-Cre
BRCA1f/fp53+/-
anti-
EGFR
anti-
ALDH1
100 µm
D
Erlotinib
(µM)
0
0.2
0.5
1
2
10
Cre-neg
MMTV-Cre
BRCA1f/f
MMTV-Cre
BRCA1f/f
p53+/-
0.1 mm

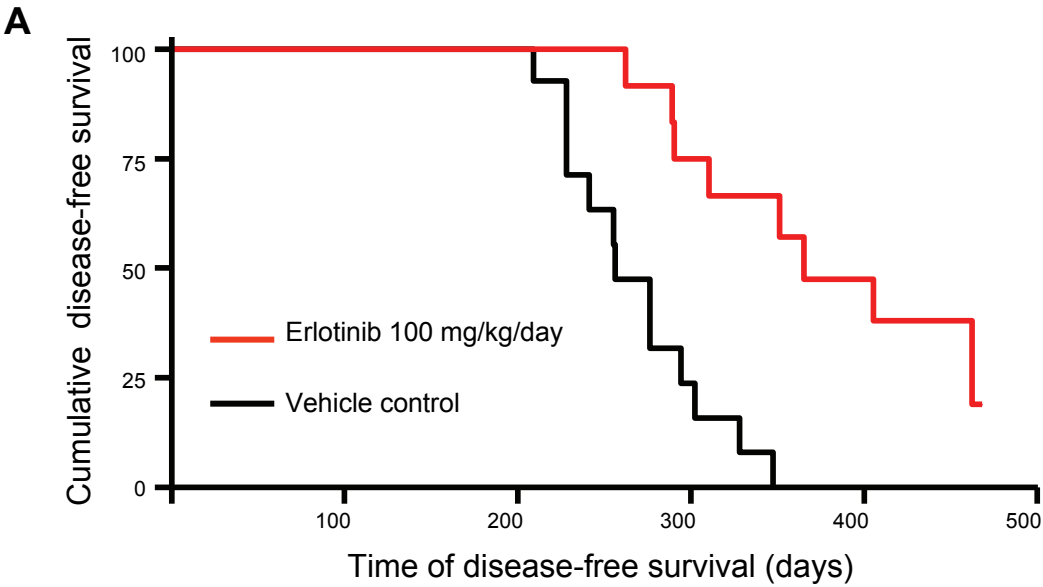
A
Cumulative disease-free survival
100
75
50
25
0
Erlotinib 100 mg/kg/day
Vehicle control
100
200
300
400
500
Time of disease-free survival (days)

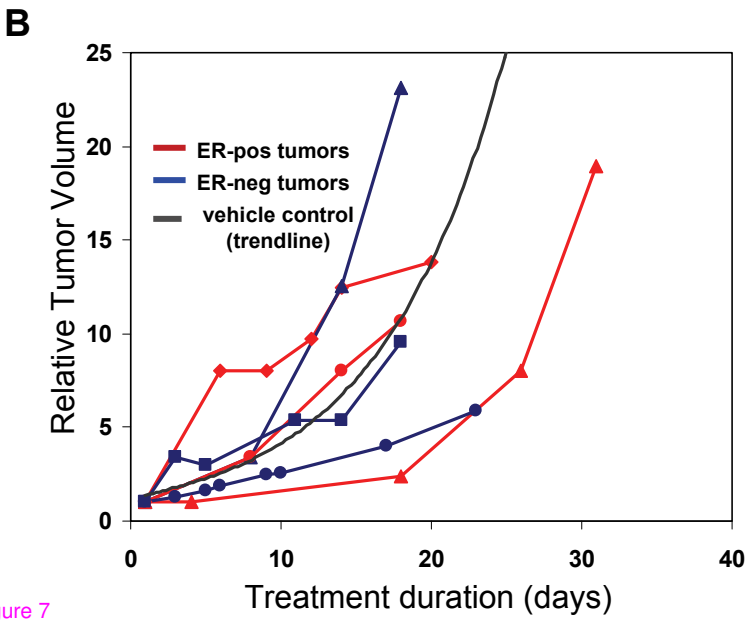
B
Relative Tumor Volume
25
20
15
10
5
0
ER-pos tumors
ER-neg tumors
vehicle control
(trendline)
0
10
20
30
40
Treatment duration (days)

Figure 7

Additional files provided with this submission:

Additional file 1: supplemental Fig. 1.pdf, 310K
http://breast-cancer-research.com/imedia/6654082045053419/supp1.pdf
Additional file 2: supplemental Fig. 2.pdf, 2835K
http://breast-cancer-research.com/imedia/1783424620505341/supp2.pdf